



UNIVERSITI
TEKNOLOGI
MARA

Journal of Mechanical Engineering

An International Journal

Volume 10 No. 2

December 2013

ISSN 1823-5514

Simulation of Flow around a Flapping Wing
Using Two-dimensional Vortex Method

Akhmad Farid Widodo
Lavi Rizki Zuhail
Hari Muhammad

Material Characterization and Axial Crushing Tests of Single
and Double-Walled Columns at Intermediate Strain Rates

Leonardo Gunawan
Sahril Afandi Sitompul
Tatacipta Dirgantara
Ichsan Serya Putra
Hoon Huh

Stability Augmentation for Longitudinal Modes of a
Small Blended Wing-Body Aircraft with Canard
as Control Surface

Rizal E. M. Nasir
Wahyu Kuntjoro

Experimental Cooling Mode Variation of an
Air-Cooled Pem Fuel Cell Using Second-Order
Thermal Analysis

Wan Ahmad Najmi Wan Mohamed
Rahim Atan

Ballistic Resistance Analysis of Non-filled Tank
against Fragment Simulating Projectile (FSP)

MR. Aziz
W. Kuntjoro
NV. David
R. Ahmad

JOURNAL OF MECHANICAL ENGINEERING (JMechE)

EDITORIAL BOARD

EDITOR IN CHIEF:

Professor Wahyu Kuntjoro – Universiti
Teknologi MARA, Malaysia

EDITORIAL BOARD:

Professor Ahmed Jaffar – Universiti
Teknologi MARA, Malaysia
Professor Bodo Heimann – Leibniz
University of Hannover Germany
Dr. Yongki Go Tiau Hiong – Nanyang
Technological University, Singapore
Professor Mirosław L. Wyszynski –
University of Birmingham, UK
Professor Ahmad Kamal Ariffin Mohd Ihsan
– UKM Malaysia
Professor P. N. Rao, University of Northern
Iowa, USA
Professor Abdul Rahman Omar – Universiti
Teknologi MARA, Malaysia
Professor Masahiro Ohka – Nagoya
University, Japan
Datuk Professor Ow Chee Sheng – Universiti
Teknologi MARA, Malaysia
Professor Yongtae Do – Daegu University,
Korea
Dr. Ahmad Azlan Mat Isa – Universiti
Teknologi MARA, Malaysia
Professor Ichsan S. Putra – Bandung Institute
of Technology, Indonesia

Dr. Salmiah Kasolang – Universiti Teknologi
MARA, Malaysia
Dr. Mohd. Afian Omar – SIRIM Malaysia
Professor Darius Gnanaraj Solomon –
Karunya University, India
Professor Mohamad Nor Berhan – Universiti
Teknologi MARA, Malaysia
Professor Bernd Schwarze – University of
Applied Science, Osnabrueck, Germany
Dr. Rahim Atan – Universiti Teknologi
MARA, Malaysia
Professor Wirachman Wisnoe – Universiti
Teknologi MARA, Malaysia
Dr. Thomas Ward – University of Malaya,
Malaysia
Dr. Faqir Gul – Institute Technology Brunei,
Brunei Darussalam
Dr. Valliyappan David a/l Natarajan –
Universiti Teknologi MARA, Malaysia

EDITORIAL EXECUTIVE:

Dr. Koay Mei Hyie
Rosnadiyah Bahsan
Farrahshaida Mohd. Salleh
Mohamad Mazwan Mahat
Nurul Hayati Abdul Halim

Copyright © 2013 by the Faculty of Mechanical Engineering (FKM), Universiti Teknologi MARA, 40450 Shah Alam, Selangor, Malaysia.

All rights reserved. No part of this publication may be reproduced, stored in a retrieval system, or transmitted in any form or any means, electronic, mechanical, photocopying, recording or otherwise, without prior permission, in writing, from the publisher.

Journal of Mechanical Engineering (ISSN 1823-5514) is published by the Faculty of Mechanical Engineering (FKM) and UiTM Press, Universiti Teknologi MARA, 40450 Shah Alam, Selangor, Malaysia.

The views, opinions and technical recommendations expressed herein are those of individual researchers and authors and do not necessarily reflect the views of the Faculty or the University.

Journal of Mechanical Engineering

An International Journal

Volume 10 No. 2

December 2013

ISSN 1823-5514

1. Simulation of Flow around a Flapping Wing Using Two-dimensional Vortex Method 1
Akhmad Farid Widodo
Lavi Rizki Zuhul
Hari Muhammad
2. Material Characterization and Axial Crushing Tests of Single and Double-Walled Columns at Intermediate Strain Rates 19
Leonardo Gunawan
Sahril Afandi Sitompul
Tatacipta Dirgantara
Ichsan Setya Putra
Hoon Huh
3. Stability Augmentation for Longitudinal Modes of a Small Blended Wing-Body Aircraft with Canard as Control Surface 37
Rizal E. M. Nasir
Wahyu Kuntjoro
4. Experimental Cooling Mode Variation of an Air-Cooled Pem Fuel Cell Using Second-Order Thermal Analysis 53
Wan Ahmad Najmi Wan Mohamed
Rahim Atan

5. Ballistic Resistance Analysis of Non-filled Tank against Fragment
Simulating Projectile (FSP)

75

MR. Aziz

W. Kuntjoro

NV. David

R. Ahmad

Experimental Cooling Mode Variation of an Air-Cooled Pem Fuel Cell Using Second-Order Thermal Analysis

*Wan Ahmad Najmi Wan Mohamed
Rahim Atan
Faculty of Mechanical Engineering,
Universiti Teknologi MARA
40450 Shah Alam, Selangor, Malaysia.*

ABSTRACT

Thermal analysis of air-cooled Polymer Electrolyte Membrane (PEM) fuel cells for closed cathode designs are largely limited within first-order thermal analysis. Normally, closed cathode fuel cells apply the water cooling technique due to large cooling loads. Technical feasibility study in applying air cooling as an alternative for closed cathode stack designs is reported here using a down-scaled 3-cell stack assembly. A 242 cm² active area, 3-cell closed cathode PEM fuel cell stack, was developed with 40 integrated straight path air cooling channels in order to investigate the internal thermal effects. The objective is to identify the bulk thermal effects of the stack under cooling for further design considerations using the second-order thermal analysis approach. Tests were conducted with airflows in the range between 200 and 400 Reynolds number and load variations from 10A to 30A. Different fan settings are applied to analyze the response of the design to negative and positive pressure airflows. The temperature profiles are translated into stack cooling profiles with discussions on its polarization, cooling response behaviour and cooling effectiveness. Generally, the cooling effectiveness across all cooling modes was higher than 80% and the negative pressure fan setting provides a more consistent cooling profile but with a slower cooling response.

Keywords: *Fuel cells, air cooling, cooling effectiveness, thermal engineering.*

Introduction

Air cooling is applied in both open cathode and closed cathode Polymer Electrolyte Membrane (PEM) fuel cell designs. Open cathode PEM fuel cells concurrently utilizes the reactant air as a heat sink and cooling agent. It depends heavily on environmental conditions where the humidity of the surrounding air directly affects the stack performance [1]. Open cathode designs are currently limited to 1 kWe, and are mostly suitable for miniature PEM fuel cells application such as micro-aerial and demo-scale vehicles, robots, small power systems, and communication electronics [2]. On the other hand, closed cathode designs, which can now reach modular outputs beyond 100 kW, appropriately require adequate active cooling assistance to maintain the cells at a suitable operating temperature. The current practice in PEM fuel cells thermal management is the application of air-cooled system for low output range, sub kW to 2 kW systems, and using water-cooled system for higher output ranges. However, Faghri and Guo [3] stated that cells operating between 2 kW and 10 kW may still apply air cooling through judicious decision makings, undoubtedly both in design and operation.

Technically, thermal engineering is the application of suitable cooling techniques to control the stack temperature within its operating limit. Specifically, it serves to maintain a high uniformity of temperature profile in the porous gas diffusion layer [4]. It is an operational requirement and closely related to the water management aspect; however, individual studies are possible whenever the selected analytical domain is intentionally detached from the electrochemical reactions. One such domain is the design of cooling systems. As a rule, the application of active cooling systems is compulsory for fuel cells above the 100W power output.

Commercialization and interest of fuel cells has just aggressively started at the turn of the century, and apart from full-scale car prototype developments, PEM fuel cell stacks with power outputs less than 3 kW are much in demand. The popular applications include backup power systems and small-scale or demonstration vehicles, mainly conducted by research institutions and academia. From this initial culture, there is a potential market for small-sized PEMFC stacks with power output ratings of up to 3 kW. The main advantage air cooling systems holds over water-cooled systems is that it is more compact, increasing the overall system size by usually less than 50%, whereas water-cooled systems generally increases the system size by more than 200%. Therefore, for portable and limited space applications, air-cooled fuel cells are very much desirable.

Thermal Engineering of Air-cooled PEM Fuel Cells

Physical investigation on the thermal effects of air cooling for stacks in the range of 1 kW to 3 kW power rating is rare compared to publications on water-cooled systems. The majority of predictive modeling concerning stack power outputs, temperature profiles and cooling effects are obtained largely from analytical approach, built from the foundations of theoretical electrochemistry, species transport and heat transfer. However, it is acknowledged that actual fuel cell behavior is also specifically influenced by component, manufacturing and assembly methods such as clamping pressure distribution and sealing characteristics, as well as flow disturbances due to MEA deflection and imperfections in gas channel construction. In other words, each developed PEM fuel cell would actually exhibit its own unique operational signature.

The academic assumption where a fuel cell operates similarly every single time is certainly considered to be too idealistic. The uniqueness of a fuel cell behaviour mainly comes from the factors affecting reaction kinetics on the catalyst layers which are too sensitive to microscopic changes causing heterogeneous surface reaction occurrence [5]. Active sites require faster cooling rates to maintain near uniform cell temperatures. Wen and Huang [6] acknowledged the importance of identifying the hot spots as a vital step towards effective cooling and uniform cell temperatures.

The sensitivity of PEM fuel cell stacks to temperature is generally linked to the moisture levels required in the membrane for positive charge transport across the electrodes. Heat buildup within the cells would quickly dry the membrane and leads to greater electrical and thermal resistances [7]. However, heat is also needed for improved reaction kinetics at the catalyst layers. Therefore, thermal management of PEM fuel cells has to balance both requirements.

Part of the experimental and analytical approach in this paper is adopted from the works of various researchers. Zhang et al. [8] introduced the lumped thermal mass model applying the transient stack temperature profiles based on solid-state thermal analysis. Temperature profile plots at different load currents and dynamic temperature to electrical power variation were identified as useful tools in modeling and experimentally validating steady-state and dynamic heat transfers in a stack [9]. The methodology for internal stack temperature measurements was shown in [10] with focus on cooling response analysis. Effect on stack-fan configuration to the performance of a fuel cell was conducted by Sasmitho et al. [11], but all of these techniques are still constrained within the first-order thermal analysis.

First-order thermal analysis directly relates the temperature measurements to the bulk characteristics of the system. However, second-order analysis allows an improved understanding on the internal thermal behaviour of the stack, i.e. the rate of heat gain and dissipation in response to electrical power and cooling

mode variations. From the calculated cooling rate, qualitative analysis on the effectiveness of the cooling operations can be performed [12]. Hence, a detailed cooling analysis of an air-cooled PEMFC under dynamic operational settings is the main subject presented here. The operational relationship between a certain design of mini channel geometry to differences in fan operation, in this case the application of positive and negative flow pressures, was reported together with a detailed methodology for the evaluation of cooling effectiveness from the perspective of second-order thermal analysis. In addition, thermal engineering studies on air-cooled closed cathode fuel cells are very rare compared to studies on open cathode stacks [13,14].

Thermal Analysis

Thermal analysis from the perspective of fluid-solid interaction, or convection, is a difficult science in terms of accuracy. Disturbances in fluid flow, transient surface temperatures, or dynamic cooling loads usually pose a major problem in properly determining the representative heat transfer coefficient. Solid state thermal analysis via conduction is more direct and poses little problem in reliability even at dynamic load conditions [8].

Transient thermal behavior is more complex due to the ever-changing boundary conditions of the system such as the surface temperature. In actual fuel cell operation, dynamic local reactions are common due to factors such as localized mass concentration, membrane humidity changes and perturbations in reactant flow. In a solid body with heat generation and internal cooling, temperature changes will continue to occur exponentially until an asymptotic thermal saturation level, or a steady-state temperature distribution is reached [15]. This saturation level is a result of conductive and convective rate equilibrium which is reached within a specific time period and dependent on the specific temperature gradient within the solid, the convective cooling coefficient development and cooling surface geometries. The common method in transient conduction analysis of a system under cooling is the lumped capacitance method. However, its accuracy depends on the magnitude of temperature gradients within the solid body.

The usual analytical methodology regarding thermal analysis of air-cooled PEM fuel cells is as reported in [16]; stack temperatures is directly interpreted in various aspects to determine the impact of the cooling mode. Conversion of the physical measurements into a second order internal properties such as cooling rates are rarely found. In this work, the determination of various convective cooling properties is not a viable approach as the system involves a fuel cell stack with a set of cooling channels. Variations in cooling air parameters such as inlet velocity, flow rate, and even temperature is expected in the individual channels due to the fan-stack configuration. As dynamic

reaction sites are also expected across the cells, application of the lumped capacitance method in this study is also too complex to achieve. Therefore, empirical solid state analysis was taken as the analytical methodology for cooling performance evaluation.

Despite operating based on the principles of electrochemical rather than thermochemical reactions, a PEM fuel cell generates heat as a by-product of the reaction irreversibilities, exothermic formation of water vapor and the ohmic resistances on charge flow across the electrodes. For simplicity, the heat generated within fuel cells are assumed to be the heat generated mainly at the reaction sites of the cathodes due to water vapour formation. The amount of heat generated can be estimated by using the system relations [17] based on the energy balance of the system and depending on the state of water formed.

Energy of the fuel = electrical power obtained + heat generated

$$\frac{I}{n.F} H_{fuel} \cdot n_{cell} = I.V_{cell} \cdot n_{cell} + Q_{gen} \quad (1)$$

Normally, the water exists as vapor, and so the heating value of the fuel is equal to the Lower Heating value, and consequently

$$Q_{gen} = (1.254 - V_{cell}) I.n_{cell} \quad (\text{Watts}) \quad (2)$$

The required cooling load of individual cooling channels can be determined through

$$Q_{ch} = \frac{P_{th,cell}}{n} = \frac{(V_{rev} - V_{cell}) I_{cell}}{n} \quad (\text{Watts}) \quad (3)$$

$$\eta_{cell} = \frac{V_{cell}}{V_{rev}} \quad (4)$$

The reversible cell voltage, V_{rev} , is the maximum thermodynamically calculated potential of a single fuel cell regardless of size and design. It is evaluated based on the heating value of the fuel (hydrogen) and relative to the water phase formed during oxidation. Using the Lower Heating Value (LHV), a value of 1.254V is obtained. The theoretical cell voltage, V_{cell}^0 , at any current loadings can be estimated by applying the conversion efficiency relation. In experiments, the measured cell voltage and current are directly applied to obtain the cell efficiency, η_{cell} , and thermal load. The total stack thermal load is calculated by substituting the cell voltage with the total stack voltage, and multiplying the reversible cell voltage with the appropriate number of cells.

In available literature concerning experimental approach, the common analysis relates the external stack temperatures to the phenomena under study. While this is a satisfactory approach to meet the required objectives, the evaluation of internal heat transfer rates would provide deeper insight on the thermal behavior of the cells. Transient temperature profiles are accompanied by its respective transient cooling rate profiles that clearly indicates the energy balance within the stack.

In experimental design, the internal stack temperature is continuously monitored in time steps. The temperature profiles can be converted into transient heat transfer plots based on

$$\Delta Q_{stack, gain} = \frac{m_{cg} C_{cg} (T_{i+2} - T_i)}{\Delta t} \quad (\text{Watts}) \quad (5)$$

where:

- $\Delta Q_{stack, gain}$: change of stack heat content for the duration of the time step (W)
- m_{cg} : total mass of carbon graphite plates (kg)
- C_{cg} : specific heat of carbon graphite (J/kg.K)
- T_i : temperature reading at initial time step (K)
- T_{i+1} : temperature reading at end of single time step (K)
- Δt : time step (sec)

The transient heat transfer profile is an indicator for the rate of thermal energy change within the measured periodicals; a positive value points to stack heating effect while negative values indicates a cooling effect. From the analysis of the experiments, the transient plots were shown to exhibit an exponential behavior with negative gradient and so requiring an arithmetically averaged heat transfer values for steady-state performance evaluation purposes such as the determination of the cooling effectiveness.

$$\Delta Q_{stack, avg} = \frac{m_{cg} C_{cg} (T_{i+n} - T_i)}{\Sigma t} \quad (\text{Watts}) \quad (6)$$

where:

- $\Delta Q_{stack, avg}$: averaged stack heat change rate (W)
- T_i : initial temperature reading (K)
- T_{i+n} : temperature reading at end of operation (K)
- Σt : total operation time (sec)

Evaluation of cooling effectiveness is central in any thermal cooling systems. Here, the cooling effectiveness is a direct comparison between the averaged cooling rates of the stack to the thermal power generated during operation.

$$\varepsilon = \frac{Q_{c, avg}}{P_{th, stack}} \quad (7)$$

where the average cooling rate, $Q_{c, avg}$ is obtained by subtracting the generated thermal power (P_{th}) at each loading to the arithmetically evaluated averaged stack energy change ($Q_{stack, avg}$).

$$Q_{c, avg} = P_{th} - Q_{stack, avg} \quad (\text{Watts}) \quad (8)$$

The cooling effectiveness is relative to the simultaneous conditions of generated thermal power of the stack at a particular load and the rate of stack heating or energy gain; higher heating effect does not directly translate to lower cooling effectiveness.

PEM Fuel Cell Design and Experimental

Stack Design

A 3-cell PEM assembly was developed with a nominal plate size of 330 cm² and half plate dimensions as shown in Figure 2. The cooling channels, labelled as Ms40, are of straight path configuration with an aspect ratio of 1.7 (3.48 mm width x 2 mm height). A single bipolar plate consists of 40 integrated cooling channels that runs through the plate with a total running length of 149.5 mm per channel. There are two bipolar plates and two monopolar plates in the 3-cell assembly. It should be noted that the monopolar plates does not integrate any cooling channels.

The reactant flow field designs for both anode and cathode of the bipolar plate are multipass serpentine channel configuration with different number of channels, as specified in Table 1. In a fuel cell, the Membrane Electrode Assembly (MEA) is the heart of the cell where the electrochemical reaction occurs. The 5 layered MEA has an active area of 242 cm² per cell, making it a large sized fuel cell by definition.

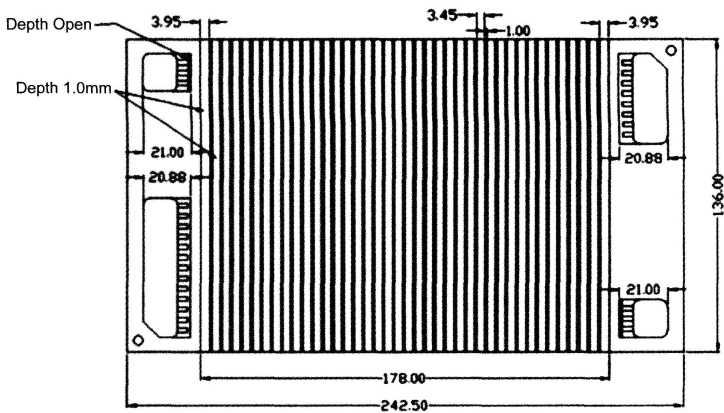


Figure 2. Half section geometry of the bipolar plate showing the integrated cooling channels within the plate

Table 1. General specifications of the flow field design

Specification	Anode	Cathode
Single channel geometry	Width : 1 mm Depth: 0.5 mm	Width : 1 to 2 mm Depth: 0.5 mm
Flow configuration	7-pass serpentine	3-pass serpentine
Number of nominal channels	24	15
Total area coverage	240 cm ²	240 cm ²

Experimental

The experimental objective was to investigate the thermal characteristics of the cooling channel design based on solid-state thermal analysis. To obtain the cooling effectiveness of each design, the heating and cooling rates of the stack are required which are directly dependant on the stack temperature profile. The heating rate can also be linked to its overall polarization behavior and calculated using equation 2; therefore, the stack voltage has to be monitored across all current loadings where the overall power curve of the stack is statistically determined. In turn, the cooling rates were obtained by the changes in the enthalpy of the stack; hence, an averaged stack temperature needs to be presented from a set of temperature readings across the stack.

Thermocouples were positioned within the cooling channels, approximately 25 mm from the open ends, to obtain a direct surface temperature

response to the cooling activity. The positioning covered both cooling fluid ends within three designated stack zones relative to the hydrogen inlet and outlet ports – top zone (near the hydrogen inlet), middle zone and bottom zone (near the hydrogen exit) – as illustrated in Figure 4.

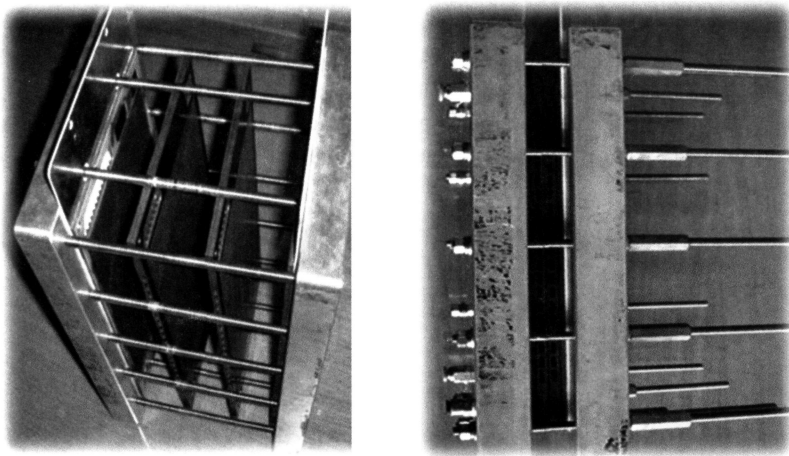


Figure 3. Stack assembly (left) and side view (right) displaying the internal components and the integrated cooling channels within the two bipolar plates

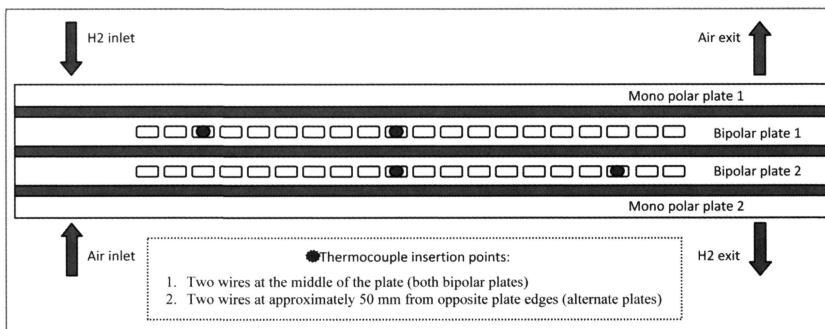


Figure 4. Schematic showing the positioning of the thermocouples at one end of the stack; thermocouple depth at 25 mm from open ends

In order to limit the effects of reactant-assisted cooling, the experiments exercised external parameter control by applying constant stoichiometric ratios (adjustments to mass flow) and using non-humidified reactants. A novel aspect of this work is on conducting the tests under different fan settings. Typically, the cooling fans are set at negative pressure (or suction) and positioned horizontally

to induce air flow from the bottom to the top of the stack. Cooling effects at positive pressure flows was not found in literature. Here, the fans are positioned vertically (as in Figure 5) and two fan settings were applied based on varying the flow momentum sources (positive and negative pressures). Four fans, with a power rating of 6W each (refer Table 2 for specifications), are mounted on a plate covering the entire cooling channel array and forming a single cooling fan system.

Three current loadings of 10A, 20A and 30A were applied for each fan setting. It is essential in having at least three data points (load variation) at each fan setting for the predictive mathematical application. This provides a variation in stack performance database (I-V curves) that was further processed

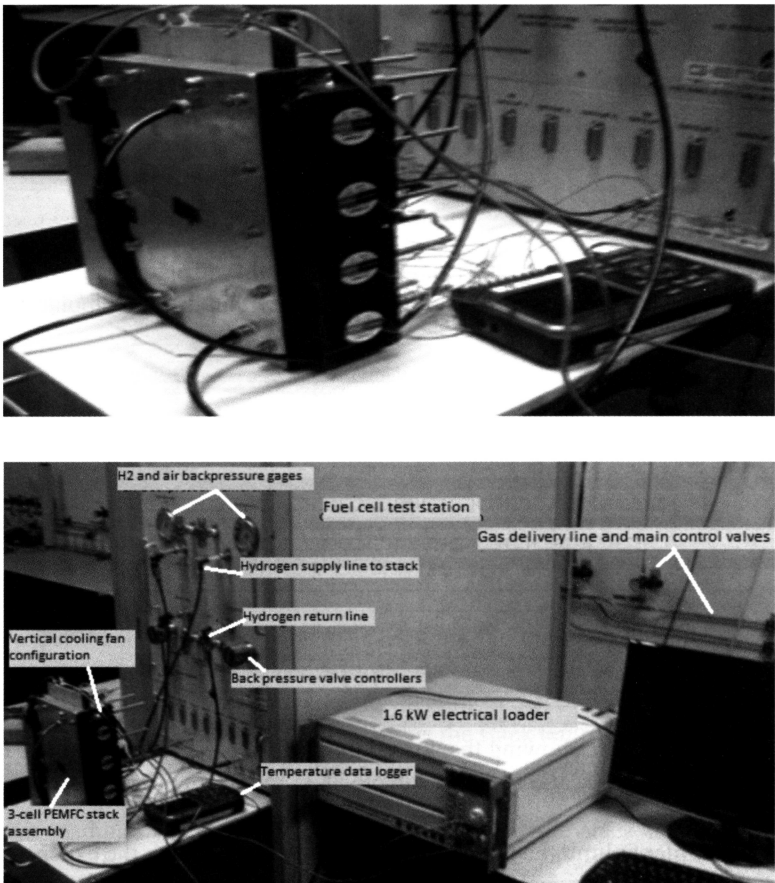


Figure 5. Actual experimental setup inclusive of fuel cell stack, test station, reactant supply lines, and data acquisition facilities

by statistical analysis to obtain a generalized polarization behavior with higher accuracy.

The test sets were labeled based on both the load and fan setting. The first letter designates the cooling fan setting and the immediate number identifies the current load setting, as specified in Table 3. Three sets of measurement instruments installed. The first were the cables connecting both electrodes with the electrical loader that allows load control and measurement of stack voltage. The second set was thermocouple wires positioned within the cooling channels. The third set was a multi meter for manual cell voltage monitoring

Table 2. Cooling fan specifications

Parameter	Value
Model type	EC-6025HH12C
Input power (max speed)	4.6W
Voltage DC	12V
Overall size (casing)	120 mm x 120 mm
Fan speed	6000
Air flow at max fan speed	31.81 CFM

Table 3. Designation of test labels based on load and fan setting

Load (Amp)	Cooling fan setting	
	Blower (B)	Suction (C)
10	B10A	C10A
20	B20A	C20A
30	B30A	C30A

At each load, the test station automatically updates the voltage values over a standard 5 second interval. Temperature monitoring were performed by the temperature data logger, also manually set at 5 second intervals. Besides the total stack voltage, individual cell voltages were measured manually using the multi meter. Each individual tests were performed at 10 minutes of active load and cooling as the stack thermal equilibrium were normally reached within

that period; less time at lower loads. The internal properties of the fuel cell material is provided in Table 4 and were applied in the analytical methodology. The specification of the experimental parameters is listed in Tables 5 to 8.

Table 4. PEMFC stack parameters

Properties / parameters	Values
1. Material	Carbon graphite
2. Specific heat, C	710 J/kg.K
3. Density	2240 kg/m ³
4. Top/bottom surface areas (total)	57.12 cm ²
5. Side surface areas (total)	1018.5 cm ²
6. Thermal conductivity	20 W/m.K

Table 5. Experimental setup parameters

Properties / parameters	Values
1. Load current	10A, 20A and 30A
2. Test station model	GasHub 1.6 kW
3. Temperature data logger model	Gavitron
4. Number of temperature probes	8 K-type thermocouple wires

Table 6. Cooling air supply properties

Properties / parameters	Values
1. Inlet temperature (ambient)	26°C – 29°C
2. Nominal velocity at max fan power	
- Blower fan setting	2.2 m/s
- Suction fan setting	1.9 m/s

Table 7. Hydrogen supply properties

Properties / parameters	Values
1. Delivery pressure from main line	0.8 bar gage
2. Inlet pressure	0.6 bar – 0.7 bar gage
3. Backpressure difference	0.2 bar – 0.4 bar gage
4. Inlet temperature	32°C – 35°C
5. Supply flow rate range (stoichiometry)	
- 10A load	0.9 l/min (12)
- 20A load	1.3 l/min (8.7)
- 30A load	1.5 l/min (6.7)
6. Supply source	Hydrogen supply tank
7. Purity	99.999%

Table 8. Reactant air supply properties

Oxygen (Air)	
Properties / parameters	Values
1. Delivery pressure from mainline	1 bar gage
2. Inlet pressure	0.7 bar – 0.8 bar gage
3. Backpressure difference	0.2 bar – 0.4 bar gage
4. Inlet temperature	35°C – 38°C
5. Supply flow rate	0.24 liters/min
6. Air stoichiometry	
- 10A load	26.4
- 20A load	13.2
- 30A load	8.8
7. Supply source	Compressed air tank
8. Relative humidity	≈ 50%

Results and Discussion

The experimental results and analysis are presented here in the order of stack polarization, stack temperatures, transient and steady-state cooling rates and cooling effectiveness.

Stack Polarization

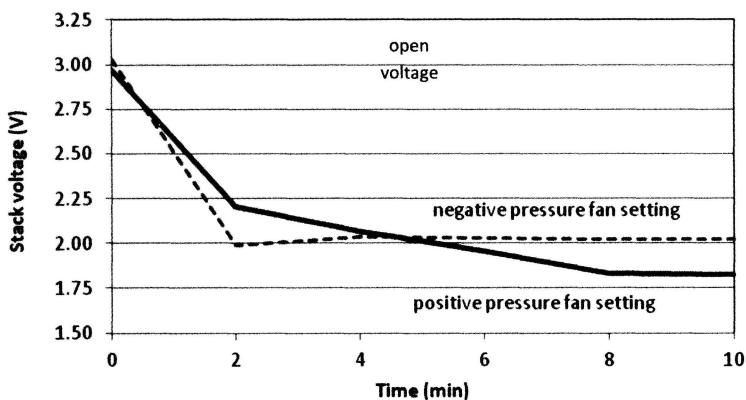


Figure 6. Example of averaged stack voltage profiles (at 10A loading) showing the existing variations during experimental

Throughout the different loadings, there were slight variations in stack voltages of both fan settings (Figure 6) due to differences in reactant flow and subsequent cell activity. Figure 7 is an example of the averaged stack voltage profile based on the individual cell voltage readings, and these averaged values were applied extensively for the determination of subsequent electrical and thermal analysis. To evaluate its statistical reliability, standard deviation analysis of these averaged voltage values compared to the whole range of experimental values were performed. The open voltage showed the lowest standard deviation for all stacks at less than 1%, conforming the consistency of design quality and operating procedure. The maximum deviation was found under operation at 20A and 30A loads, but still falls within a very acceptable limit of less than 6%.

The normalized I-V curves using averaged voltage values and the ensuing electrical-thermal power outputs are presented in Figures 8 and 9. As an important note, all stacks were operated at reactant temperatures near to ambient as well as low inlet pressures. In addition, the performance was based on dry reactant condition where no humidification of the reactants was performed. These operating conditions were selected to evaluate the thermal

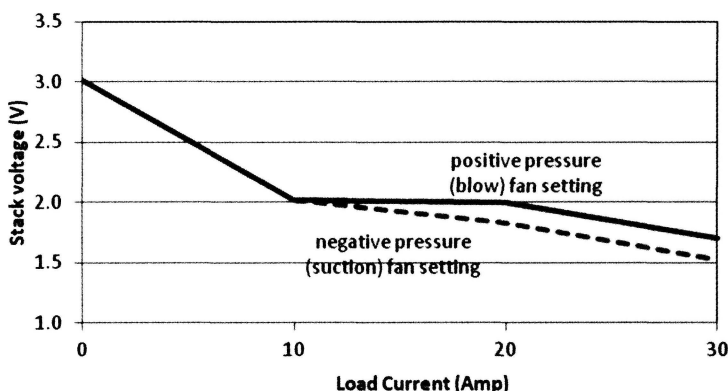


Figure 7. Averaged voltage variation for both fan settings

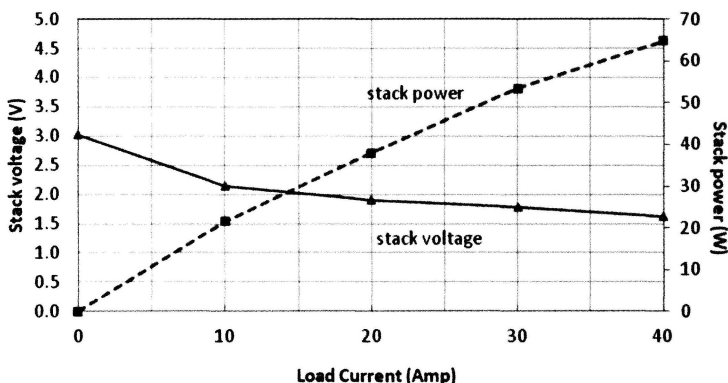


Figure 8. Normalized I-V curves of stack Ms40 from no load to 40A electrical load

effects within the stack without significant influence from the inherent reactant properties. However, the selected operating conditions led to lower power densities than usually obtained for industrial stacks.

The polarization analysis allows the evaluation of thermal energy as the load is varied. It is closely related to the conversion efficiency which is determined from the actual stack voltage changes. Equal electrical and thermal power outputs occurs at approximately 20A load corresponding to a conversion efficiency of 50%. From that point onwards, the thermal power increases exponentially compared to the reduced rate of electrical power rise as the efficiency falls below 50%. The maximum thermal-to-electrical power ratio at 40A was determined at 1.3 to 1.

Fuel cell voltage is relatively dependant on the energy density of each reactant flowing through the anode and cathode, as well as the conductivity of the

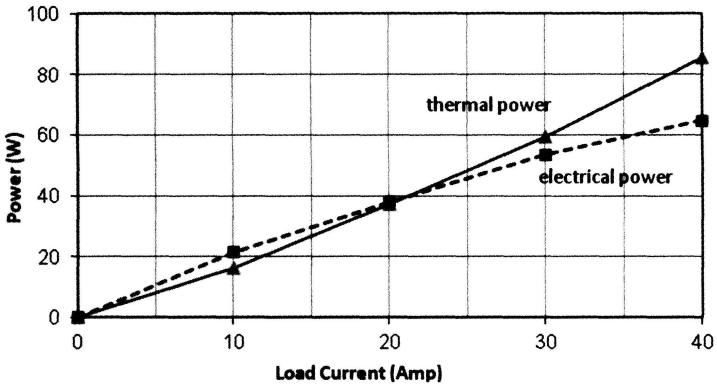


Figure 9. Electrical and thermal power generation (50% cell efficiency at 20A load)

components bridging the two reactants. At its maximum voltage (open voltage condition), the electrons are not flowing resulting in optimum energy density difference between the opposite polars. When the circuit between anode and cathode is connected and electrical load is demanded, electrochemical activity at both anode and cathode converts the reactants into its respective compounds, and so the mass and energy density of the reactants were reduced resulting in the energy equilibrium being compromised.

An efficient fuel cell (high voltage at high load current) allows a very fast removal and replenishment of the reactants. However, the existence of generated heat and water, and combined with geometrical aspects of the flow channels such as depth and length that influences the mechanics of flow, would have diverse effects on the rate of reactant replenishment into the fuel cell. The most common phenomena during operation to explain voltage drops would be the flooding effect, which is caused by formation of water in liquid phase within the channels and blocking the passage of reactants. Operation at low reactant temperature, such as defined for the works here, evidently promoted a high level of flooding within the channels that led to voltage deteriorations.

Stack Temperature

In active cooling experiments, the zonal stack temperatures for each experimental set were individually plotted, as presented in Figure 10 for blower fan setting at 20A load, allowing a closer look into the temperature distribution along a cooling channel at a specified zone as well as an indicator on areas of electrochemical activity. However, these zonal temperatures are individual readings and do not represent the stack temperature as a lumped entity. Therefore, the temperature

readings were averaged to represent a single stack temperature as a basis for thermal calculations.

The middle zone profile indicates that the center area temperature is always higher than the exit area temperature. The inlet area temperatures, where cooling effects are optimum due to first contact with the incoming coolant, are significantly lower than the exit temperature. The trend found here highly suggests that the center area is actively generating heat. Further details on active reaction zone characterization are beyond the scope of this publication and will be presented elsewhere.

The comparative profiles of the averaged stack temperature (Figure 11) indicates a greater cooling consistency of the negative pressure (suction) fan setting compared to positive pressure (blow) setting due to a better degree of flow control into the channels. Higher inlet resistance are expected from the more energetic and mixed fluid stream of the blower fan setting resulting in lower flow rates within the cooling channels. At 30A load where the stack thermal energy is generated higher and across a wider MEA area, the blower fan setting has the advantage of stack edge cooling that contributed to enhanced cooling rates.

In terms of cooling response, the suction fan setting has the capability to achieve thermal saturation conditions at a faster response time compared to blower fan setting, especially at low thermal loads. However, a significant increase in generated thermal energy (at 30A) shows that the cooling response deteriorates for the suction fan setting and is approximately similar with the blower fan setting. In general, the controlled induced streamlines of the suction fan setting provides a more stable cooling behavior within the channels.

Cooling Profile and Effectiveness

The averaged stack temperature profile is the representative bulk temperature of the stack as it is simultaneously heated and cooled. At varying loads, difference in generated thermal power was observed. The relation between the generated stack heat, assumed constant for a specific electrical load, and the stack heat gain profile provided the required dynamic cooling rates of each load and fan setting. Due to the constant thermal power assumption (P_{th}), the projected transient cooling trend ($Q_{c, transient}$) resembles the trend of the exponential stack energy gain ($Q_{stack, exp}$), but with a visible difference in magnitude and flow vector (minus sign indicating stack cooling). Mathematically,

$$Q_{c, transient} = P_{th} - Q_{stack, exp} \quad (Watts) \quad (9)$$

In Figure 12, the relationship is presented graphically based on the load 30A of the positive pressure fan setting. With an assumed constant generate heat, the stack thermal gain was initially higher as the energy is accumulated and reduces exponentially as the cooling effect kicks in. By subtracting the

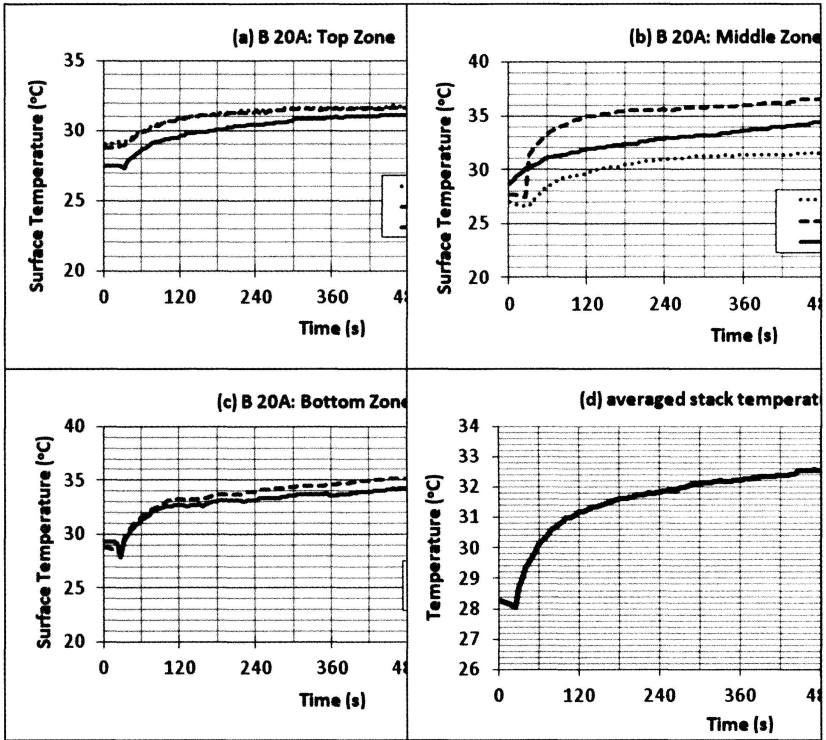


Figure 10. Stack temperature profiling at different stack zones (a - c) while (d) is the averaged stack temperature (data from 20A load and full power blower fan setting experimental).

stack heat gain from the generated heat, a cooling profile was obtained. The cooling trendline is similar to the stack heat gain trend due to the assumed linear heat generation.

An effective cooling system is capable of immediately responding to the cooling load that would translate into lower temperature jumps and thus reducing the effect of thermal stresses within the fuel cell. The exponential cooling rate trend should also have a large negative gradient that allows the conduction and convective heat transfer mechanisms to reach an asymptotic level at a faster response time. Figure 13 compares the cooling profiles of all the experimentations, and it shows a larger gradient is generally achieved by the suction fan setting.

Generally, the cooling effectiveness of all the modes are at acceptable levels. An excellent cooling system should reach at least 90% cooling effectiveness. Figure 13 indicates that this requirement is partially achieved.

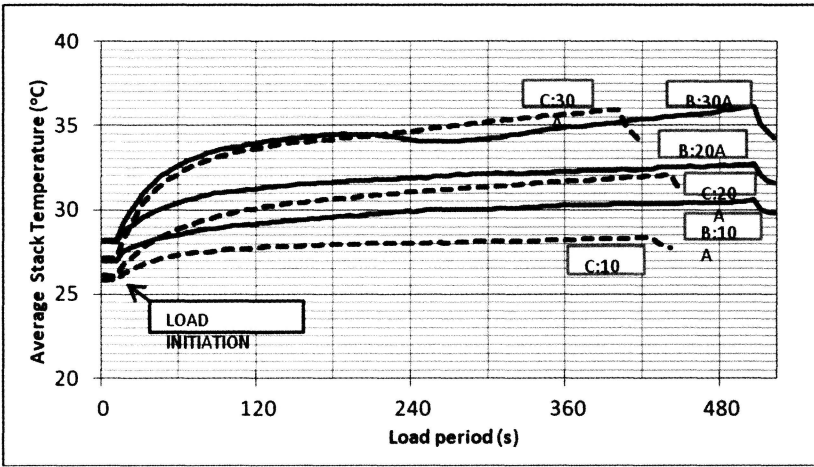


Figure 11. Averaged stack temperature profile across all electrical loads (B: positive pressure fan setting; C: negative pressure)

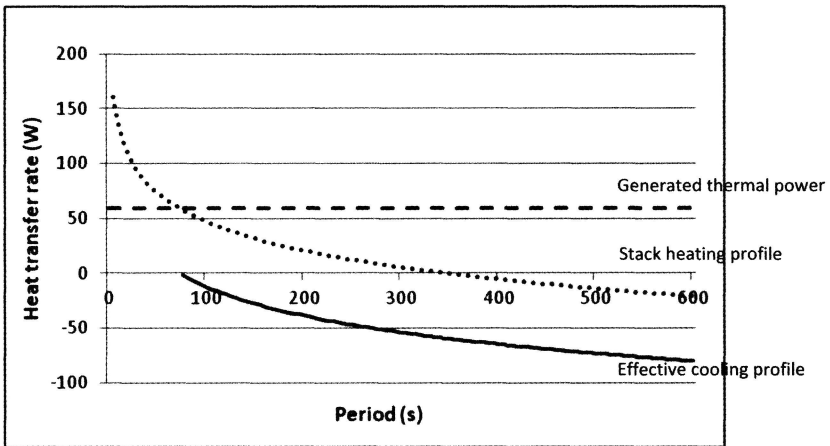


Figure 12. Graphical presentation of the transient cooling rate of the stack based on a constant heat generation (from blower fan setting at 30A)

In terms of cooling consistency, a difference of 6% between the minimum and maximum effectiveness was obtained. The effectiveness of negative pressure fan setting (suction) is slightly lower than its positive pressure counterpart, but, it is able to provide a higher consistency (2% difference across all loads). The slightly higher cooling performance of the blower fan setting is mainly due to the assistance of frontal surface cooling which is negligible for its counterpart.

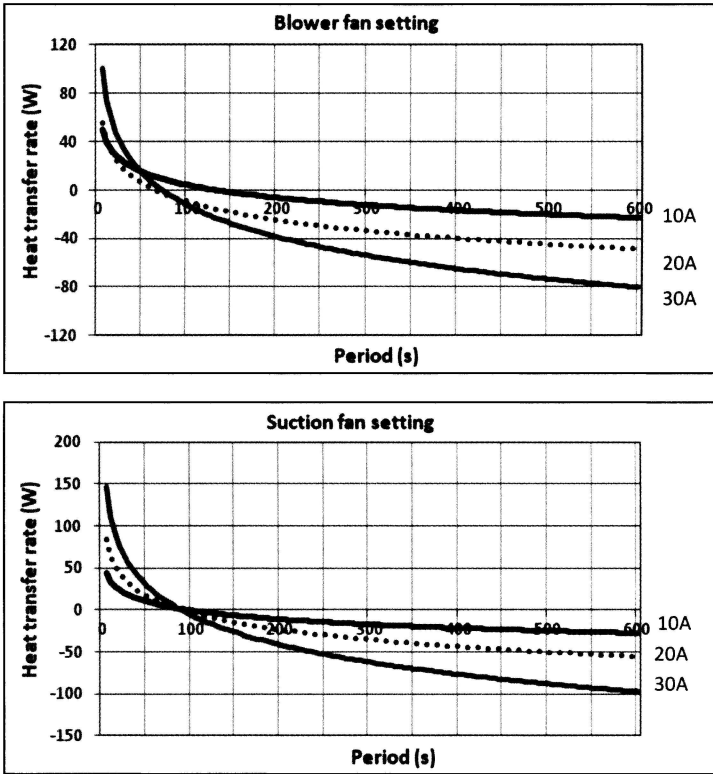


Figure 13. Cooling profile for both suction and blower fan settings across all the loads

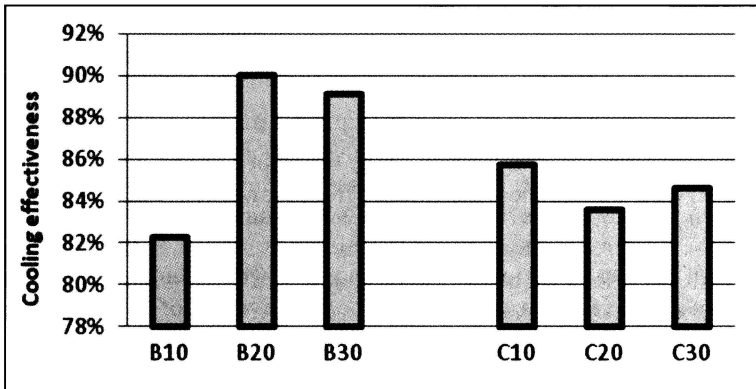


Figure 14. Cooling effectiveness of each operating mode based on averaged cooling rate

The erratic, but satisfactory, cooling performance is largely due to its smaller channel aspect ratio which gives a higher resistance to incoming fluid flow. However, smaller cross-sections provide an ideal heat transfer interaction between the hot surface and the cooling fluid, partially offsetting the effect of inlet resistance.

Conclusion

Experimental investigation on the effect of cooling modes to the thermal behaviour of a PEM fuel cell stack was performed. The methodology for second-order thermal analysis was outlined and provided more information on the cooling effectiveness of the thermal management operation compared to conventional first-order stack temperature analysis. Though the variations in cooling effectiveness values was not literally translated into a fixed temperature difference between the cooling modes, the general trend where high cooling effectiveness points to lower maximum stack temperatures are evident. Thermal saturation condition between the conduction and convection mechanisms within the stack governs the cooling response and effectiveness of each cooling mode. It was also found that the stack accumulates heat load for periods of no less than four minutes before the cooling effects and its distribution stabilizes the stack temperature. The accumulated heat load would cause thermal stresses and expansion of components, leading to concentrated leaks as well as permanent deformation such as cracks.

References

- [1] Chu, D. and Jiang, R. (1999). "Performance of PEMFC stacks, Part I. Evaluation and simulation of an air-breathing PEMFC stack," *J. Power Sources*, 83: 128-133.
- [2] Chen-Yu Chena, Wei-Hsiang Lai, Biing-Jyh Weng, Huey-Jan Chuang, Ching-Yuan Hsieh, and Chien-Chih Kung, (2008). "Planar array stack design aided by rapid prototyping in development of air-breathing PEMFC," *J. Power Sources*, 179: 147-154.
- [3] Faghri, A. and Guo, Z. (2005). "Challenges and opportunities of thermal management issues related to fuel cell technology and modelling," *International Journal of Heat and Mass Transfer*, 48: 3891-3920 (2005).
- [4] Perng, S.-W. and Wu, H.-W. (2009). "Heat transfer in a PEMFC flow channel," *Applied Thermal Engineering*, 29: 3579-3594.
- [5] Hasmady, S., Fushinobu, K. and Okazaki, K. (2007) "Treatment of heterogeneous electrocatalysis in modelling transport-reaction phenomena in polymer electrolyte fuel cells," in *Proceedings of the International*

Networking for Young Scientists from the United Kingdom and Malaysia in Renewable Energy Technology, UKM Bangi, Malaysia.

- [6] Wen, C.-Y. and Huang, G.-W. (2008). "Application of a thermally conductive pyrolytic graphite sheet to thermal management of a PEM fuel cell," *J. Power Sources*, 178: 132-140.
- [7] W. A. Najmi W. M. and Atan, R. (2012). "Analysis of Stack Heating on the Thermal and Electrical Resistance Characteristics of Polymer Electrolyte Membrane Fuel Cell", *International Journal of Automotive and Mechanical Engineering (IJAME)* 5: 648-659.
- [8] Zhang, Y., Ouyang, M., Lu, Q., Luo, J. and Li, X. (2004). "A model predicting performance of PEM fuel cell stack thermal system," *Applied Thermal Engineering*, 24: 501-513.
- [9] Graf, C., Vath, A. and Nicoloso, N. (2006). "Modeling of the heat transfer in a portable PEFC system within MATLAB-Simulink," *J. Power Sources*, 155: 52-59.
- [10] Adzakpa, K.P., Ramousse, J., Dubé, Y., Akremi, H., Agbossou, K., Dostie, M., Poulin, A. and Fournier, M. (2008). "Transient air cooling thermal modelling of a PEM fuel cell," *J. Power Sources*, 179: 164-176.
- [11] Sasmito, A.P., Birgersson, E., Lum, K.W. and Mujumdar, A.S. (2012). "Fan selection and stack design for open-cathode polymer electrolyte fuel cell stacks", *Renewable Energy*, 37(1): 325-332.
- [12] W. A. Najmi W. M. and Atan, R. (2013). "Stack Cooling Profile of an Air-Cooled 3-Cell Polymer Electrolyte Membrane Fuel Cell Stack", *Applied Mechanics and Materials*, 393: 774-780.
- [13] Sasmito, A.P., Birgersson, E. and Mujumdar, A.S. (2012). "A Novel Flow Reversal Concept for Improved Thermal Management in Polymer Electrolyte Fuel Cell Stacks", *International Journal of Thermal Sciences*, 54: 242-252.
- [14] Sasmito, A.P., Shamim, T., Birgersson, E. and Mujumdar, A.S. (2013). "Numerical Investigation of Water and Temperature Distributions for Open-Cathode Polymer Electrolyte Fuel Cell Stack with Edge Cooling", *Journal of Fuel Cell Science and Technology*, 10(6): doi:10.1115/1.4025054.
- [15] Incropera, F. P. and DeWitt, D. P. (2002). *Fundamentals of Heat and Mass Transfer*, Fifth Edition. John Wiley & Sons, 240-243.
- [16] Matian, M., Marquis, A. and Brandon, N. (2011). "Model based design and test of cooling plates for an air-cooled PEM fuel cell stack," *International Journal of Hydrogen Energy*, 36: 6051-6066.
- [17] Spiegel, C.S. (2007). *Designing and building fuel cells*, McGraw Hill USA.